Bull. Chem. Soc. Ethiop. **2024**, 38(2), 527-538.
DOI: https://dx.doi.org/10.4314/bcse.v38i2.19

ISSN 1011-3924
Printed in Ethiopia
Online ISSN 1726-801X

SPECTROSCOPIC, PHYSICOCHEMICAL CHARACTERIZATIONS AND PHOTONICS APPLICATIONS ON BORON SUBPHTHALOCYANINE CHLORIDE AS ORGANIC ELECTRONICS

Arwa Alrooqi[1,2], Amal A. Alshehri[2], Zahra M. Al-Amshany[1], Laila M. Al-Harbi[1], Tariq A. Altalhi[3], Moamen S. Refat[3*], A.A. Atta[4], Gaber A. M. Mersal[3], A.M. Hassanien[5] and Kareem A. Asla[6]

[1]Department of Chemistry, Faculty of Sciences, King Abdulaziz University, P.O. Box 80203, Jeddah 21589, Saudi Arabia
[2]Department of Chemistry, Faculty of Arts and Science, Al-Baha University, Baljurashi, Saudi Arabia
[3]Department of Chemistry, College of Science, Taif University, P.O. Box 11099, Taif 21944, Saudi Arabia
[4]Department of Physics, College of Science, Taif University, P.O. Box 11099, Taif 21944, Saudi Arabia
[5]Department of Physics, College of Science and Humanities, Shaqra University, Al Quwaiiyah, Saudi Arabia
[6]Department of Chemistry, Faculty of Science, Zagazig University, Zagazig, 44519, Egypt

(Received October 9, 2023; Revised November 24, 2023; Accepted November 28, 2023)

ABSTRACT. This work shows the structural, thermogravimetric, optical, and electrochemical properties of boron subphthalocyanine chloride (B-subPc-Cl) as organic electronic material. The Fullprof Suite program and Rietveld analysis were used to refine and index the crystal structure of B-subPc-Cl. The thermogravimetric analysis (TGA) and the differential thermogravimetric analysis (dTG) were used to study the kinetic thermogravimetric factors using the Horowitz-Metzger's and Coats-Redfern methods. The absorption spectra of B-subPc-Cl contain two strong absorption bands (Soret-like band and Q-like band). The oscillator strength and electrical dipole strength were estimated by using a Gaussian fitting of the molar absorptivity (ε_{molar}) of the B-subPc-Cl. The HOMO-LUMO and the band gap of B-subPc-Cl were calculated by using cyclic voltammetry measurement. Details of the UV-Vis – NIR absorption spectra and optical band gap for B-subPc-Cl are also provided. Density-functional theory (DFT) method has been utilized to obtain geometrically optimized structure for the studied compound. The theoretical calculations agreed with the experimental results. The obtained results point out the prospects of B-subPc-Cl for the organic electronic applications.

KEY WORDS: Subphthalocyanine, Optical properties, TGA, Cyclic voltammetry, DFT method

INTRODUCTION

Recently, the great developments of optoelectronic and microelectronics technologies based on small molecules of organic semiconductors have been achieved because they enjoy unique physicochemical properties. Organic small molecules containing conjugated π- electron systems can be used as functional materials in numerous fields of organic electronic devices [1, 2]. Within the great class of porphyrinoid structures, phthalocyanines enjoy an advantaged position in charge management and electronic devices [3, 4]. Phthalocyanines have found extensive use in materials science research and progressively more in various and significant technological and industrial areas. They play a variety of roles in modern material science technology such as photovoltaic solar cells, semiconductor devices, and nanobiotechnology [5-7]. Subphthalocyanines are a famous class of dyes and pigments that have applications organic optoelectronic devices [2].

*Corresponding author. E-mail: moamen@tu.edu.sa ; msrefat@yahoo.com

Subphthalocyanines are non-planar macro-heterocyclic organic compounds containing three isoindole structures assembled around tetrahedral boron(III) center, which bears group (typically aryloxy) or halogen atom in the axial position. Subphthalocyanines have higher solubility compared to phthalocyanines [2]. Boron subphthalocyanine chloride (B-subPc-Cl) is a non-planar cone structure that is recognized as a donor material in organic solar cells [8]. It has 14 delocalized π-electrons with excellent optical and physical properties [9]. B-subPc-Cl organic molecule shows a strong dipole moment oriented along the B–Cl direction [10]. A boron subphthalocyanine chloride dye is formed from the chemical reaction between phthalonitrile and BCl_3 in aromatic solvents such as p-xylene or toluene [11]. Recently, Morse *et al.* [12] reported that the B-subPc-Cl possesses many desirable characteristics such as intense and narrow absorbance, an intense and narrow orange fluorescence, low sublimation temperatures, tunable electronic properties. For potential uses of B-subPc-Cl dye in materials science research and industrial areas, structural, electrochemical, and optical spectroscopic studies on B-subPc-Cl were done.

EXPERIMENTAL

Chemicals and instrumentals

Boron subphthalocyanine chloride ($C_{24}H_{12}BClN_6$) organic compound with a molecular weight of 430.7 g/mol was purchased from Sigma-Aldrich Chem. Co. The crystal structure of the B-subPc-Cl was explored at room temperature by using Philip X-ray diffractometer with Cu Kα radiation with a scan speed of 2 degrees/minute. The thermogravimetric analysis (TGA) and differential thermogravimetric analysis (dTG) of the B-subPc-Cl dye were simultaneously measured by the Shimadzu DTG-60H thermal analyzers at a single (10 °C/min) and heating rate (30 °C/min). Sample mass 4.5 mg and Al_2O_3 as a reference were non-isothermally heated in nitrogen flow (20 mL/min) from 25 to 800 °C. The quantitative data were estimated from the relevant TGA curve to determine the kinetic parameters for all the B-subPc-Cl dye at a single heating rate (10 °C/min) by the Coats-Redfern [13] and Horowitz-Metzger's [14] methods. The absorbance spectra were obtained on the Cary series UV-Vis–NIR spectrophotometer (Agilent Technologies). The UV-Vis–NIR spectra were measured over the range of 200-800 nm. All the spectra were obtained at room temperature in dimethyl sulfoxide (DMSO) as a solvent and quartz cells with a path length of 1 cm. An Autolab potentiostat PGSTAT 302 (Eco Chemie, Utrecht, Netherlands) was used to perform cyclic voltammetry (CV). A carbon paste electrode (working electrode), Ag/AgCl (reference electrode), and platinum wire (counter electrode) were used in the electrochemical cell. A Metrohom pH-meter with a combined glass electrode was used to calculate the pH values. The pH values were modified using a solution of 1 M NaOH.

Theoretical studies

Computational studies were performed using $DMOL^3$ program [15] in Materials Studio package [16]. DFT semi-core pseudopods calculations (dspp) were done with the double numerica basis sets as well as polarization functional (DNP) [17]. The RPBE functional is based on the generalized gradient approximation (GGA) as best correlation functional [18, 19].

RESULTS AND DISCUSSION

Physical assignments

The Fullprof Suite program (2020) is used to analyze and refine XRD data to determine the phase structure and the lattice parameters of B-subPc-Cl based on the Rietveld method and a pseudo-

Voigt function (Figure 1). The geometrical structure was drawn using the VESTA-win64 software. This analysis shows that B-subPc-Cl has an orthorhombic structure with: Pnma (#62-1) space group and lattice parameters; a = 12.07860 Å, b = 14.79890 Å, c = 10.23490 Å, α = β = γ = 90° and crystal volume (V = 1829.4883 Å^3). During the Rietveld structure refinement of the structure under study, the Wyckoff positions and asymmetric unit for the various space groups were applied [20]. The lattice parameters; a ≈ ap $\sqrt{2}$, $b \approx a_p$, *and* $c \approx a_p \sqrt{2}$ were utilized for the orthorhombic phase with P_{nma} space group. The examination of the TGA and dTG curves reveals that the investigated B-subPc-Cl dye decomposes with two degradation steps. The corresponding dTG data (385 and 471 °C) reveals that the decomposition processes of this dye are thermally endothermic. In general, the rapidity of this dye decomposition process can be described as slow. In B-subPc-Cl dye, the mass losses (73.10%) in the first and second steps were attributed to the elimination of $C_{21}H_{12}ClN$ molecule (cal. 73.06%) endothermally. Therefore, the dye B-subPc-Cl exhibited a high decomposition temperature (385 °C), probably due to its highest structural steric hindrance. The residue left in the crucible consists of Beta carbon nitride (β-C_3N_4) which is a superhard material predicted to be harder than diamond [21]. Boron nitride ceramic has excellent chemical and thermal stability and can be used as a part of high-temperature equipment. Horowitz-Metzger's and Coats-Redfern [13, 14] equations were used to determine the kinetic thermogravimetric factors of B-subPc-Cl. The kinetic thermogravimetric factors such as free energy change of the decomposition (ΔG^*), enthalpy (ΔH^*) can be estimated by applying the Horowitz-Metzger's and Coats-Redfern [13, 14]. The kinetic thermogravimetric parameters of the decomposition steps such as E^*, Â, ΔS^*, ΔH^*, and $\Delta G^*$are estimated and tabulated in the Table 1.

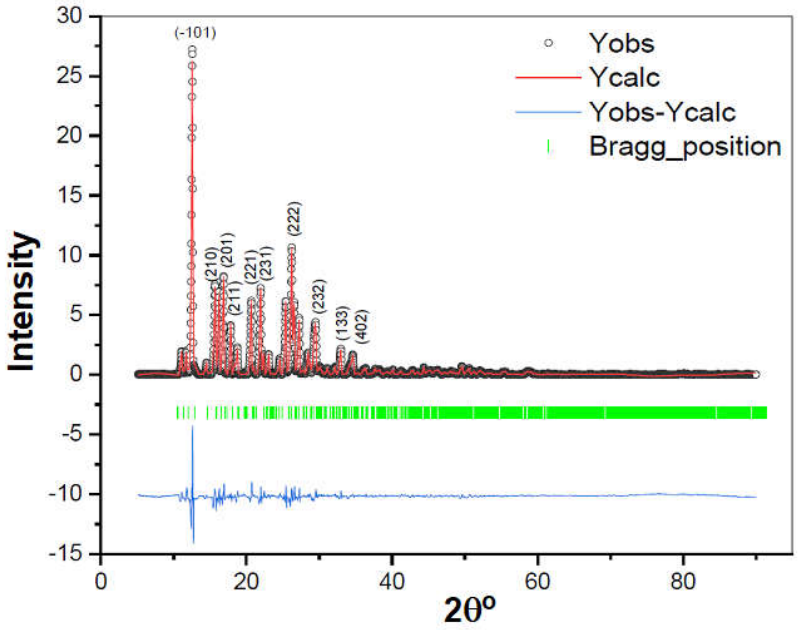

Figure 1. X-ray diffraction patterns (Y_{obs}) and the refined pattern using the Rietveld method (Y_{calc}) for B-subPc-Cl dye.

Table 1. Kinetic thermodynamic parameters of B-subPc-Cl dye.

Methods	dTG/Max	E^*	ΔH^*	ΔS^*	ΔG^*	Â
Coats-Redfern	471	2.61E+05	2.55E+05	-6.58E+01	2.07E+05	0.9495
Horowitz-Metzger's	471	2.96E+05	2.90E+05	-1.17E+02	2.04E+05	0.9369

The obtained kinetic thermogravimetric parameters indicate that the B-subPc-Cl has thermal stability and is more appropriate from the economic viewpoint [22-24]. B-subPc-Cl contains delocalized 14 π-electrons structure that provides rise to strong absorption bands in the UV-Vis region.

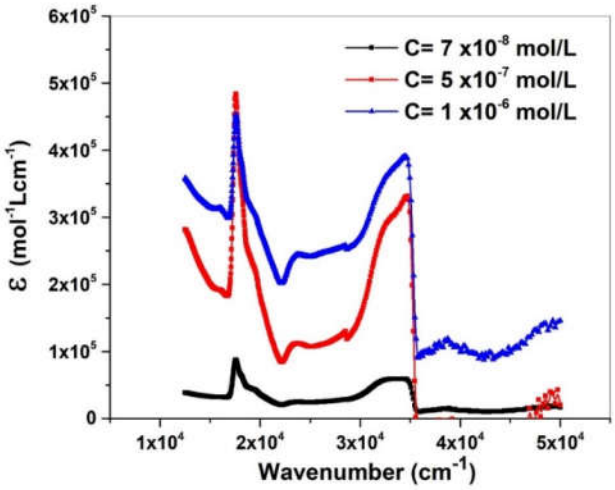

Figure 2. Spectral behavior of the molar absorptivity (ε_{molar}) for B-subPc-Cl in DMSO with different concentrations.

Figure 2 shows spectral behavior of the molar absorptivity (ε_{molar}) for B-subPc-Cl in dimethyl sulfoxide (DMSO) with concentrations 7×10^{-8} mol/L, 5×10^{-7} mol/L, and 1×10^{-6} mol/L at room temperature (~300 K). The figure shows the B-subPc-Cl has a strong absorption band in the near UV (Soret-like band) at 288 nm and a strong absorption (Q-like band) at 567 nm. Morse *et al.* [12] reported that the Q-band, is seen generally between 560−600 nm equating to an optical band gap of 2.1−2.0 eV. Absorption measures the amount of light of a specific wavelength that a specific substance prevents from passing through. The two essential parameters affecting absorption are the path length and the concentration of the organic dye. The higher the concentration of the organic dye, the greater its absorption, this is because the number of molecules that interact with light affects the percentage of light that is absorbed. More concentrated solutions contain a larger number of molecules that react to the entering light, thereby increasing its absorption. In a dilute solution, the absorbance is low because fewer molecules are available to interact with light. The relationship between focus and path length: the absorbance is also directly proportional to the path length, where path length refers to the distance the light travels through the material. With a longer path length, the light interacts with more molecules as it travels a longer distance through the solution. This increases absorbency. The molar absorptivity (ε_{molar}) of the B-subPc-Cl can be used to calculate the electric dipole strength (q^2) and the oscillator strengths (f) from the following relations [25-27]:

$$q^2 = \frac{1}{2500}\,\varepsilon_{molar}\,\left(\frac{\Delta\bar{\upsilon}}{\bar{\upsilon}}\right), \quad (1)$$

$$f = 4.3 \times 10^{-9} \int \varepsilon_{molar}\, d\bar{\upsilon}\ , \quad (2)$$

where $\bar{\upsilon}$ is the wavenumber and $\Delta\bar{\upsilon}$ is the absorption half band width.

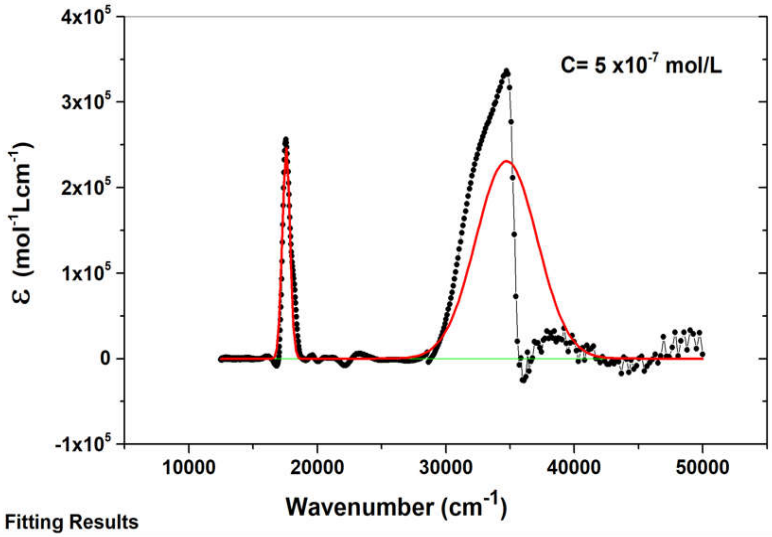

Fitting Results

Oscillator strength	Electric dipole strength	Area Intg	FWHM	Max Height	Center Grvty	Area IntgP
0.794	4.069E-8	1.83891E8	699.9922	246794.1011	17574.69244	11.75663
5.963	1.07E-8	1.38025E9	5610.79825	231101.2838	34722.22222	88.24337

Figure 3. The Gaussian fitting analysis and the calculated values of (q^2) and (f) for B-subPc-Cl in DMSO with C = 5×10^{-7} M/L.

The relation between molar absorptivity versus wavenumber for B-subPc-Cl is displayed in Figure 3. A Gaussian fitting with asymmetric least squares smoothing baseline was done to calculate *f* and q^2. The Gaussian fitting analysis and the calculated values of (q^2) and (*f*) for B-subPc-Cl in DMSO (C= 5×10^{-7} M/L) are shown in Figure 3. The UV-Vis absorption analysis can be used as a straightforward and an easy technique to precisely estimate optical band gap energies of organic π-conjugated semiconductor materials [28,29]. By using a derivation of absorption spectrum fitting (DASF), the optical bandgap of the B-subPc-Cl can be estimated. This analysis is beginning from the absorption spectrum fitting model at the absorption band edge as [30-32]:

$$A\,(\lambda) = \frac{d}{2.303}\,Z(hc)^{n-1}\lambda\left(\frac{1}{\lambda} - \frac{1}{\lambda_{gap}}\right)^n \quad (3)$$

Eq. 3 can be written as:

$$ln\left(\frac{A}{\lambda}\right) = \ln(D) + n\,ln\left(\frac{1}{\lambda} - \frac{1}{\lambda_{gap}}\right) \quad (4)$$

and then:

$$\frac{d\{ln[A(\lambda)/\lambda]\}}{d(1/\lambda)} = \frac{n}{(\frac{1}{\lambda} - \frac{1}{\lambda_{gap}})} \quad (5)$$

$$E_g^{DASF}(eV) = \frac{hc}{\lambda_{gap}} = \frac{1239.83}{\lambda_{gap}} \quad (6)$$

where A is optical absorbance, Z is a constant, c is a velocity of light, d is the film thickness and n is the power take the value of ½ for the allowed direct transition.

Figure 4 shows a relation between $\frac{d\{\ln[A(\lambda)/\lambda]\}}{d(1/\lambda)}$ and $(1/\lambda)$ for B-subPc-Cl. From this figure, the optical bandgap can be estimated as E_{gap}^{DASF} = 2.13 eV.

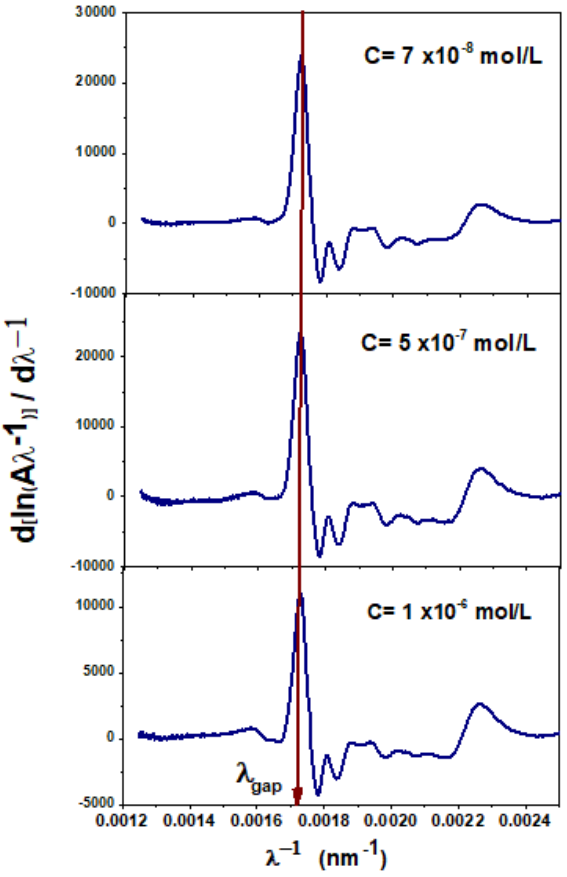

Figure 4. A relation between $\frac{d\{\ln[A(\lambda)/\lambda]\}}{d(1/\lambda)}$ and $(1/\lambda)$ for B-subPc-Cl in DMSO with different concentrations.

The electrochemical behaviour for B-subPc-Cl was investigated using cyclic voltamnmetry (CV) in dichloromethane in the presence of 0.1 M tetrabutylammonium perchlorate(TBAP) using Pt wire as a working electrode and 50 mV/s scan rate. The cyclic voltammogram for Pt electrode in the presence of B-subPc-Cl, one quasi-reversible redox systems were obtained, the oxidation peak (E_{pa1}) appeared at +0.1 V while the cathodic peak (E_{pc1}) appeared at +0.98 V. The separation of the anodic and cathodic peak potentials (ΔE) which demonstrate the reversibility behavior of the reaction, was found 20 mV. The formal potential $E_{1/2}$ was taken as the average of E_{pc1} and E_{pa1} is +0.99 V. In addition to the quasi-reversible redox system, two irreversible cathodic peaks appeared at +0.62 V and -1.13 V. The highest occupied molecular orbital (HOMO) and the lowest unoccupied molecular orbital (LUMO) energy levels were determined from their onset oxidation and reduction potentials according to the empirical relationship proposed by de Leeuw *et al.* and others [33-40].

$$E_{HOMO} = -(E_{onst\ (oxidation)} + 4.4)\ eV \quad (7)$$

$$E_{LUMO} = -(E_{onst\ (reducation} + 4.4)\ eV \quad (8)$$

The onset of oxidation $E_{(onst\ oxidation)}$ and reduction $E_{(onst\ reducation)}$ peaks are +0.97 V and -1.1 V, respectively. The calculated HOMO, LUMO and the band gap (Eg) were -5.37 eV, 3.3 eV and +2.07 eV, respectively. The ten successive cyclic voltammograms for $1x10^{-3}$ M of B-subPc-Cl have a potential range from –1.4 V to +1.4 V. By repeating the No. of cyclic voltammograms, no matched effect on the peak current of B-subPc-Cl compound was observed, which indicates that there is no absorption from B-subPc-Cl to the electrode surface and the electrode was relatively stable in DMSO solution. The effect of scan rate on the peak currents of B-subPc-Cl was examined using a wide scan rate range from 10 mV/s to 200 mV/s. As shown from Figure 5, increasing scan rate from 10 mV/s to 250 mV/s, the oxidation and reduction peak currents increased. This behavior was expected for a diffusion-controlled electron transfer process.

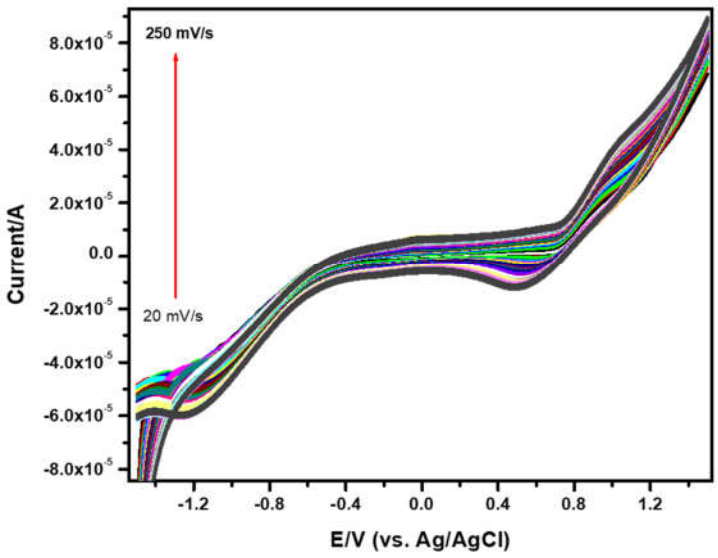

Figure 5. The effect of scan rate on the cyclic voltammogram for $1x10^{-3}$ M of B-subPc-Cl.

Molecular computational calculation

The asymmetry umbrella geometry optimization of boron subphthalocyanine dye with strong dipole moment (9.1480 D) was determined. To correlate the experimental values with the theoretical parameters, computational parameters have been computed including the energies of gas phase, frontier molecular orbitals (E_{HOMO}, E_{LUMO}), electronegativity (χ), energy band gap (ΔE) which explains the probable charge transfer interaction within the molecule, global hardness (η), chemical potential (μ), global electrophilicity index (ω) and global softness (S) [41-44] and are listed in Table 2.

Table 2. Some quantum chemical parameters of boron dye compound.

$-E_H$ (ev)	$-E_L$ (ev)	ΔE (ev)	X (ev)	μ (ev)	η (ev)	S $(ev)^{-1}$	ω (ev)	Ϭ $(ev)^{-1}$
5.128	3.548	1.580	4.338	-4.338	0.395	0.1975	23.82	2.532

The energies of both HOMO (π donor) and LUMO (π acceptor) are main parameters in quantum chemical studies. Where, HOMO is the orbital that acts as an electron donor, LUMO is the orbital that acts as the electron acceptor; and these molecular orbitals are known as the frontier molecular orbitals (FMOs). The HOMO–LUMO band gap is a good indication for compound stability [45, 46]. As HOMO–LUMO band gap increases the stability of compound increases accordingly and the chemical reactivity decreases. The significant band gap value of boron compound (ΔE_{H-L} = 1.580 eV) is agreed with the experimental indirect optical band gap after annealing. The higher values of hardness (η = 0.395) would attain a molecule higher stability according to the principle of hardness [47].

The energy components (total energy, binding energy, and dipole moment) were calculated by DFT method as shown in Table 3 for ligands. The significantly higher binding energy (B.E. = -5953 kcal/mol) revealed the higher stability of boron dye.

Table 3. Various theoretical molecular parameters of boron dye.

Dipole moment (D)	binding energy (kcal/mol)	Total energy (kcal/mol)	Zero-point vibrational energy (kcal/mol)
9.148	-5953	-1736	180.1

Vibrational calculation

The frequency calculations for boron dye were computed in vacuum, while experiments were performed for solid samples, so there are small differences between theoretical and experimental vibrational wavenumbers as shown in Figure 6. The modes of vibrations are very complex due to the low symmetry of ligands especially, in plane, out of plane and torsion modes are the most difficult to assign due to mixing with the ring modes and with the substituent modes [48]. However, there are some strong frequencies useful to characterize in the IR spectrum. The correlation graphic agreement between the theoretical and experimental wavenumbers is discussed. The relations between the calculated and experimental wavenumbers are linear for boron compound and described by the following equations:

$$\nu_{cal} = 1.00508\ \nu_{Exp} - 1.07077 \quad \text{with} \quad R^2 = 0.99989 \tag{9}$$

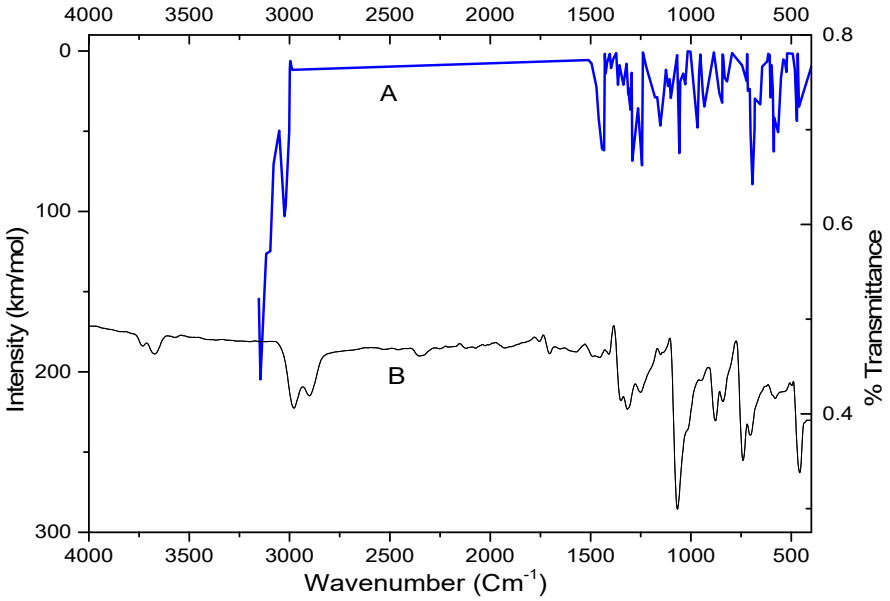

Figure 6. Comparison of theoretical (A) and experimental (B) IR spectra of boron dye.

Molecular electrostatic potential (MEP)

The electrostatic potential V(r) at a given point r(x, y, z) is defined in terms of the interaction energy between the electrical charge generated from the molecule electrons, nuclei and proton located at (r) [49, 50]. Computation of electrostatic potential is possible for molecules using the Γ-point and multiple k-points. As can be seen from MEP map, the regions of negative potential are over the electronegative atoms (carbon and nitrogen atoms) while the regions having the positive potential are over the (boron and hydrogen atoms).

CONCLUSION

The crystal structure of the B-subPc-Cl has an orthorhombic structure with Pnma (#62-1) space group and lattice parameters a = 12.07860 Å, b = 14.79890 Å, c = 10.23490 Å, α = β = γ = 90° and crystal volume (V = 1829.4883 Å^3). The kinetic thermogravimetric parameters obtained from the Coats-Redfern and Horowitz-Metzger's equations indicate that the B-subPc-Cl has thermal stability and is more appropriate from the economic viewpoint. B-subPc-Cl has two absorption bands at 288 nm (Soret-like band) and 567 nm (Q-like band). The Gaussian fitting analysis was used to obtain the oscillator strength and the electrical dipole strength. The optical bandgap ($E_{gap}^{DASF} = 2.13\ eV$ of the B-subPc-Cl in dimethyl sulfoxide (DMSO) as a solvent was estimated from a derivation of absorption spectrum fitting (DASF) method. Cyclic voltammetry measurement was used to calculate HOMO (-5.37 eV), LUMO (3.3 eV), and the band gap (E_g = 2.07 eV). The significant band gap value of boron compound ($\Delta E_{H\text{-}L}$ = 1.580 eV) is agreed with the experimental indirect optical band gap after annealing. The higher values of hardness (η = 0.395) would attain a molecule higher stability according to the principle of hardness. The

obtained results are vital for the applications into applied scientific research fields such as optoelectronics and organic electronics.

ACKNOWLEDGEMENTS

The researchers would like to acknowledge Deanship of Scientific Research, Taif University for funding this work.

REFERENCES

1. Qin, J.; An, C.; Zhang, J.; Ma, K.; Yang, Y.; Zhang, T.; Li, S.; Xian, K.; Cui, Y.; Tang, Y.; Ma, W.; Yao, H.; Zhang, S.; Xu, B.; He, C.; Hou, J. 15.3% efficiency all-small-molecule organic solar cells enabled by symmetric phenyl substitution. *Sci. China Mater*. **2020**, 63, 1142-1150.
2. Skvortsov, I.A.; Kovkova, U.P.; Zhabanov, Y.A.; Khodov, I.A.; Somov, N.V.; Pakhomov, G.L.; Stuzhin, P.A. Subphthalocyanine-type dye with enhanced electron affinity: Effect of combined azasubstitution and peripheral chlorination. *Dyes Pigm*. **2021**, 185, 108944.
3. Bottari, G.; Torre, G.; Guidi, D.M.; Torres, T. An exciting twenty-year journey exploring porphyrinoid-based photo- and electro-active systems. *Coord. Chem. Rev*. **2021**, 428, 213605.
4. Swarts, P.J.; Pieter, J.C. Electrochemical behaviour of chloro- and hydroxysubphthalocyanines. *Electrochim. Acta* **2020**, 329, 135165.
5. Zorlu, Y.; Dumoulin, F.; Bouchu, D.; Ahsen, V.; Lafont, D. Lafont, Monoglycoconjugated water-soluble phthalocyanines. Design and synthesis of potential selectively targeting PDT photosensitisers. *Tetrahedron Lett*. **2010**, 51, 6615-6618.
6. Gounden, D.; Nombona, N.; van Zyl, W.E. Recent advances in phthalocyanines for chemical sensor, non-linear optics (NLO) and energy storage applications. *Coord. Chem. Rev*. **2020**, 420, 213359.
7. Fu, Q.; Zhang, J.; Zheng, S. Prediction of key photoelectric parameters at the interface of new subAPPC/C60 organic solar cell. *Mater. Chem. Phys*. **2020**, 255, 123616.
8. Hassanien, A.M.J. Surface topology, optical spectroscopic and electrical studies on boron subphthalocyanine chloride thin films. *Dispers. Sci. Technol*. **2022**, 43, 2134 -2141.
9. Lavarda, G.; Labella, J.; Martínez-Díaz, M.V.; Rodríguez-Morgade, M.S.; Osuka, A.; Torres, T. Recent advances in subphthalocyanines and related subporphyrinoids. *Chem. Soc. Rev*. **2022**, 51, 9482-9619.
10. Trelka, M.; Medina, A.; Écija, D.; Urban, C.; Gröning, O.; Fasel, R.; Gallego, J.M.; Claessens, C.G.; Otero, R.; Torres, T.; Miranda, R. Subphthalocyanine Based Nanocrystals. *Chem. Commun*. **2011**, 47, 9986-9988.
11. Claessens, C.G.; González-Rodríguez, D.; McCallum, C.M.; Nohr, R.S.; Schuchmann, H.P.; Torres, T. On the mechanism of boron-subphthalocyanine chloride formation. *J. Porphyr. Phthalocyanines* **2007**, 11, 181-188.
12. Morse, G.E.; Bender, T.P. Boron subphthalocyanines as organic electronic materials. *ACS Appl. Mater. Interfaces* **2012**, 4, 5055-5068.
13. Coats, A.W.; Redfern, J.P. Kinetic parameters from thermogravimetric data. *Nature* **1964**, 201, 68-68.
14. Horowitz, H.W.; Metzger, G.A. A new analysis of thermogravimetric traces. *Anal. Chem*. **1963**, 35, 1464-1468.
15. El-Rayyes, A.; Mogharbel, R.T.; Abdel-Rhman, M.H.; Ismail, M.A.; Abdel-Latif, E. Molecular geometry and biological activity of 2-(4-substituted-phenylimino)thiazolidin- 4-one compounds. *Bull. Chem. Soc. Ethiop*. **2023**, 37, 1275-1286.
16. Al-Resayes, S.I.; Jarad, A.J.; Al-Zinkee, J.M.M.; Al-Noor, T.H.; El-ajaily, M.M.; Abdalla, M.; Min, K.; Azam, M.; Mohapatra, R.K. Synthesis, characterization, antimicrobial studies,

and molecular docking studies of transition metal complexes formed from a benzothiazole-based azo ligand. *Bull. Chem. Soc. Ethiop*. **2023**, 37, 931-944.
17. Sreedevi, R.; Sinthiya, A.S.I.J.; Beaula, T.J.; Balu, T.; Murugakoothan, P. Growth, characterization and chemical computations of guanidinium trichloroacetate (GTCA) single crystal – DFT approach. *Bull. Chem. Soc. Ethiop*. **2023**, 37, 1033-1045.
18. Hehre, W.J.; Radom, L.; Schlyer, P.V.R.; Pople, J.A. *Ab Initio Molecular Orbital Theory*, Wiley: New York; **1986**.
19. Hammer, B.; Hansen, L.B.; Nrskov, J.K. Improved adsorption energetics within density-functional theory using revised Perdew-Burke-Ernzerhof functionals. *Phys. Rev. B* **1999**, 59, 7413-7421.
20. Rodriguez-Carvajal, J. Recent advances in magnetic structure determination by neutron powder diffraction. *J. Phys. B: Condens. Mater*. **1993**, 192, 55-69.
21. Ball, P. "News: Crunchy filling". Nature. doi:10.1038/news000511-1. Accessed on 5 June 2000.
22. Chang, T.C.; Wu, K.H.; Liao, C.L.; Lin, S.T.; Wang, G.P. Thermo-oxidative degradation of siloxane-containing polyimide and unmodified polyimide. *Polym. Degrad. Stab*. **1998**, 62, 299-305.
23. Borah, D.; Baruah, M.K. Kinetic and thermodynamic studies on oxidative desulphurisation of organic sulphur from Indian coal at 50–150 °C. *Fuel Process. Technol*. **2001**, 72, 83-101.
24. Siddalingaiah, A.H.M.; Naik, S.G. Spectroscopic and thermogravimetric studies on Ni(II), Cu(II) and Zn(II) complexes of di(2,6-dichlorophenyl)carbazone. *J. Mol. Struct*. **2002**, 582, 129-136.
25. Kumar, G.A.; Thomas, J.; George, N.; Kumar, B.A.; Shnan, P.R.; Poori, V.P.N.; Vallabhan, C.P.G.; Unnikrishnan, N.V. Optical absorption studies of free (H2Pc) and rare earth (RePc) phthalocyanine doped borate glasses. *Phys. Chem. Glass B* **2000**, 41, 89-93.
26. Gouterman, M. Study of the effects of substitution on the absorption spectra of porphin. *J. Chem. Phys*. **1959**, 30, 1139-1161.
27. El-Nahass, M.M.; Hassanien, A.M.; Khusayfan, N.M. Optical characterizations of thermally evaporated perylene-66 (dye content 40%) thin films. *Solid State Commun*. **2013**, 154, 51-55.
28. Costa, J.C.S.; Taveira, R.J.S.; Lima, C.F.R.A.C.; Mendes, A.; Santos, L.M.N.B.F. Optical band gaps of organic semiconductor materials. *Opt. Mater*. **2016**, 58, 51-60.
29. Hassanien, A.M.; Altalhi, T.A.; Refat, M.S.; Shakya, S.; Atta, A.A.; Alsawat, M.; Al-Hazaa, A.N.; Asla, K.A. Exploring microstructural, optical, electrical, and DFT/TD-DFT studies of boron subphthalocyanine chloride for renewable energy applications. *Optik*. **2022**, 263, 169367.
30. Souri, D.; Tahan, Z.E. A new method for the determination of optical band gap and the nature of optical transitions in semiconductors. *Appl. Phys B* **2015**, 119, 273-279.
31. Rammah, Y.S.; El-Agawany, F.I.; Mahmoud, K.A.; El-Mallawany, R.; Ilik, E.; Kilic, G. FTIR, UV–Vis–NIR spectroscopy, and gamma rays shielding competence of novel ZnO-doped vanadium borophosphate glasses. *J. Mater. Sci.: Mater. Electron.* **2020**, 31, 9099-9113.
32. Alsufyani, S.J.; Alharbi, A.N.; Atta, A.A.; Altalhi, T.A.; Refat, M.S.; Alkathiri, A.A.; Ashour, A.; Hassanien, A.M. A spectroscopic study and the effect of gamma rays on the stability and efficiency of boron subphthalocyanine dye for solar energy applications. *Radiat. Phys. Chem.* **2023**, 208, 110929.
33. de Leeuw, D.M.; Simenon, M.M.J.; Brown, A.R.; Einerhand, R.E.F. Stability of n-type doped conducting polymers and consequences for polymeric microelectronic devices. **1997**, 87, 53-59.
34. Altalhi, T.; Gobouri, A.A.; Refat, M.S.; El-Nahass, M.M.; Hassanien, A.M.; Atta, A.A.; Saad, H.A.; Alhazaa, A.N. Structural, electrochemical and optical properties of 1,2,4-triazine derivative. *Appl. Phys. A* **2020**, 126, 815.

35. Kong, Z.; Liu, D.; He, J.; Wang, X. Electrode buffer layers producing high performance nonvolatile organic write-once-read-many-times memory devices. *RSC Adv*. **2017**, 7, 13171-13176.
36. Li, J.; Zhong, H.; Liu, H.; Zhai, T.; Wang, X.; Liao, M.; Bando, Y.; Liua, R.; Zou, B. One dimensional ternary Cu–Bi–S based semiconductor nanowires: synthesis, optical and electrical properties. *J. Mater. Chem*. **2012**, 22, 17813-17819.
37. Eckhardt, H.; Shacklette, L.W.; Jen, K.Y.; Elsenbaumer, R.L. The electronic and electrochemical properties of poly (phenylene vinylenes) and poly (thienylene vinylenes): An experimental and theoretical study. *J. Chem. Phys*. **1989**, 91, 1303-1315.
38. Sun, Q.; Wang, H.; Yang, C.; Li, Y. Synthesis and electroluminescence of novel copolymers containing crown ether spacers. *J. Mater. Chem*. **2003**, 13, 800-806.
39. Mahmoudi, C.; Chouk, R.; Baatout, K.; Jaballah, N.S.; Khalfaoui, M.; Majdoub, M. Synthesis, characterization and DFT study of new anthracene-based semiconducting polyethers for OLED application. *J. Mol. Struct*. **2022**, 1251, 131993.
40. Hassanien, A.M.; Altalhi, T.A.; Atta, A.A.; AlHazaa, A.N.; Alsawat, M.; Mersal, G.A.M.; Adam, A.M.A.; Refat, M.S. Studying spectroscopic, cyclic voltammetry, and electrical properties of novel 4-amino antipyrine derivative for photonic applications. *J. Mol. Struct*. **2023**, 1272, 134201.
41. Pearson, R.G. Absolute electronegativity and hardness: applications to organic chemistry. *J. Org. Chem*. **1989**, 54, 1423-1430.
42. Geerlings, P.; De Proft, F.; Langenaeker, W. Conceptual density functional theory. *Chem. Rev*. **2003**, 103, 1793-1874.
43. Parr, R.G. Electrophilicity index. *J. Am. Chem. Soc*. **1999**, 121, 1922-1924.
44. Chattaraj, P.K.; Giri, S. Stability, reactivity, and aromaticity of compounds of a multivalent superatom. *J. Phys. Chem. A* **2007**, 111, 11116-11121.
45. Speie, G.; Csihony, J.; Whalen, A.M.; Pie-Pont, C.G. Studies on aerobic reactions of ammonia/3,5-di-tert-butylcatechol schiff-base condensation products with copper, copper(I), and copper(II). Strong copper(II)−radical ferromagnetic exchange and observations on a unique N−N coupling reaction. *Inorg. Chem*. **1996**, 35, 3519-3524.
46. Aihara, A. Reduced HOMO−LUMO gap as an index of kinetic stability for polycyclic aromatic hydrocarbons. *J. Phys. Chem. A* **1999**, 103, 7487-7495.
47. Zhou, Z.; Parr, R.G.; Garst, J.F. Absolute hardness as a measure of aromaticity. *Tetrahedron Lett*. 1988, 29, 4843-4846.
48. Lu, Y.; Wang, Y.; Jiang, Z.; Men, Y. Molecular weight dependency of surface free energy of native and stabilized crystallites in isotactic polypropylene. *ACS Macro Lett*. **2014**, 3, 1101-1105.
49. Scrocco, E.; Tomasi, J. *The Electrostatic Molecular Potential as a Tool for the Interpretation of Molecular Properties*, *New concepts II*, Springer: New York; **1973**; p 170.
50. Politzer, P.; Laurence, P.R.; Jayasuriya, K. Molecular electrostatic potentials: an effective tool for the elucidation of biochemical phenomena. *Environ. Health Perspect*. **1985**, 61, 191.